

Uplift Resistance of a Multiline Ring Anchor System in Soft Clay to Extreme Conditions

Junho Lee, S.M.ASCE¹; Krishnaveni Balakrishnan, S.M.ASCE²;
Charles P. Aubeny, Ph.D., P.E., F.ASCE³; Sanjay Arwade, Ph.D.⁴;
Don DeGroot, Sc.D., P.E., M.ASCE⁵; Alejandro Martinez, Ph.D., A.M.ASCE⁶;
and Ryan Beemer, Ph.D., A.M.ASCE⁷

¹Ph.D. Candidate, Zachry Dept. of Civil and Environmental Engineering, Texas A&M Univ., College Station, TX. Email: juno918@tamu.edu

²Ph.D. Candidate, Dept. of Civil and Environmental Engineering, Univ. of Massachusetts Amherst, Amherst, MA. Email: kbalakrishna@umass.edu

³Professor, Zachry Dept. of Civil and Environmental Engineering, Texas A&M Univ., College Station, TX. Email: caubeny@civil.tamu.edu

⁴Professor, Dept. of Civil and Environmental Engineering, Univ. of Massachusetts Amherst, Amherst, MA. Email: arwade@umass.edu

⁵Professor, Dept. of Civil and Environmental Engineering, Univ. of Massachusetts Amherst, Amherst, MA. Email: degroot@umass.edu

⁶Assistant Professor, Dept. of Civil and Environmental Engineering, Univ. of California, Davis, CA. Email: amart@ucdavis.edu

⁷Assistant Professor, Dept. of Civil and Environmental Engineering, Univ. of Massachusetts Dartmouth, Dartmouth, MA. Email: rbeemer@umassd.edu

ABSTRACT

A multiline ring anchor (MRA) system has been developed as a cost-effective alternative for securing arrays of floating offshore wind turbines (FOWTs) to the seabed. Multiline attachments can improve the economically competitiveness of FOWTs by reducing the capital cost of the support system for the floating structures. FOWTs can be subjected to severe wind and wave conditions resulting in extreme loads to the anchor system. Thus, the reliable design of the anchor system requires proper determination of the extreme mooring line loads acting on the anchor needed to secure FOWTs to the seabed. Previous studies showed the MRA in soft clay has clear advantages over existing anchors under the extreme horizontal loading conditions imposed by catenary moorings; however, its performance relative to conventional anchors under extreme vertical loading imposed by taut mooring systems requires further investigation. This study presents predictions of extreme loads on floating structures secured by taut mooring systems and evaluates the potential for developing an economical anchor for resisting these extreme loads.

INTRODUCTION

In the United States, offshore wind resource is an attractive alternative to land-based renewable resources due to its greater robustness and consistency, fewer aesthetic issues, and proximity to coastal population centers (Barter et al. 2020; Musial et al. 2016). A significant portion of offshore wind resources are located at water depths greater than 60m, where floating offshore wind turbines (FOWTs) are typically the preferred alternative over fixed platforms. One proposed concept in pursuit of cost reductions is the multiline ring anchor (MRA). The MRA comprises an embedded ring with optional wing plates and keying flaps that can be attached to enhance the load capacity (Aubeny et al. 2020, Figure 1). Multiple mooring lines (up to six) can be attached to the cylindrical

core to share the anchor, reducing the required number of anchor footprints (Figure 2), which can provide substantial reductions in site investigation, material, fabrication, and transport costs (Lee et al. 2020). The deep embedment of the MRA produces a high geotechnical efficiency (load capacity/anchor weight), enabling a smaller and lighter design relative to conventional alternatives, such as piles and caissons, and potentially substantial resistance to vertical uplift loads in catenary and taut mooring systems (Aubeny 2017; Diaz et al. 2016; Lee and Aubeny 2020).

The MRA is installable in a wide range of soil types, the scope of the present study is limited to normally consolidated clay seabed soil profiles. Previous studies showed the MRA in soft clay has clear advantages over existing anchors under the extreme horizontal loading imposed by catenary moorings (Lee and Aubeny 2020, *in press*). However, its performance relative to conventional anchors under vertical loading imposed by taut mooring systems requires further investigation. On the one hand, little doubt exists that a deeply embedded ring anchor is capable of resisting uplift loading, but the question to be addressed in this study is whether the vertical load demand from taut moorings can be resisted with anchor sizes that can be deployed using conventional vessels and handling equipment. Noting that the MRA load capacity can be enhanced either by increasing its core diameter or by adding wing plates, this paper also investigates which measure is optimal from the standpoint of minimizing fabrication and installation costs. Recent trends in FOWT design have been for larger units, going well beyond the 5-MW capacity range. This study considers loading conditions associated with a range of 5- to 10-MW units.

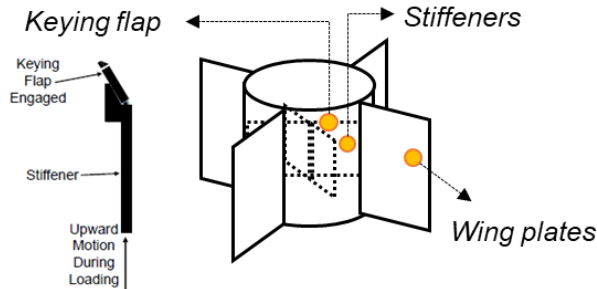


Figure 1. Strategies for enhancing load capacity (Lee and Aubeny 2020)

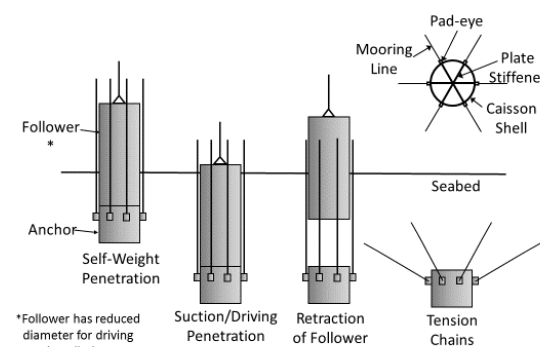


Figure 2. The installation procedure of the MRA (Lee and Aubeny 2020)

EXTREME VERTICAL LOADING

Extreme conditions and scale-up FOWTs. As the offshore wind industry has shown a tendency toward the scaled-up FOWTs and installed in deeper water, a taut mooring system can be effective means to utilize the space with better efficiency of the offshore wind farm (IEA 2019). Taut mooring systems differ from catenary mooring systems in that their mooring line does not lie down on the seabed (Figure 3). This results in relatively large tension on the mooring line relative to its submerged weight and requires utilizing a synthetic material with high elastic capacity. Additionally, severe weather conditions, such as hurricanes, induce extreme loadings to the taut mooring systems. Thus, the proper determination of the extreme mooring line load is essential for the reliable anchor design.

The capital costs of the offshore wind farm, such as foundation systems and transportation, can be significantly reduced by using the scaled-up FOWTs (Lee et al. 2020). Due to these benefits, the demand for large-sized FOWTs increases, and some scaled-up FOWTs are commercially available (Figure 4, IEA 2019). Thus, the current study also aims to evaluate the extreme mooring line load induced by the large-sized FOWTs and optimize the MRA performance under its extreme loadings.

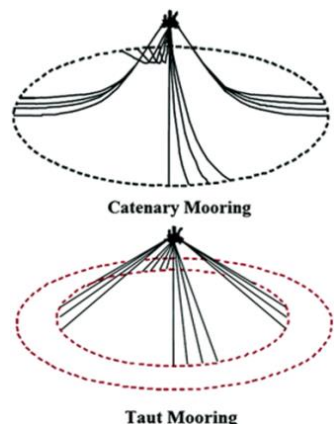


Figure 3. Catenary and taut mooring systems (Ruinen 2000)

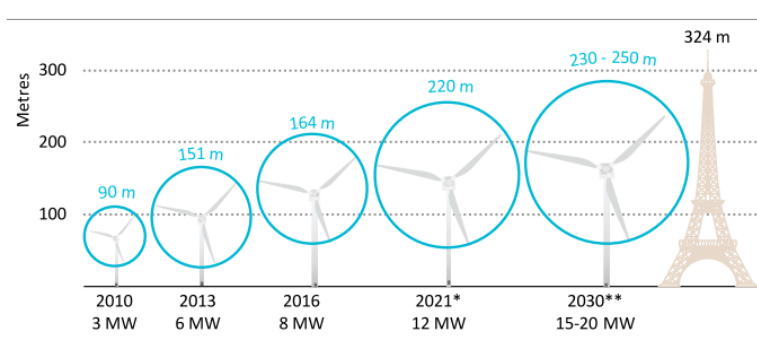


Figure 4. The evolution of the FOWTs (IEA 2019)

The multiline potential of the MRA. Fontana et al. (2018) presented that multiline (3-line) anchor force for the catenary mooring systems can be lower than that of a single-line due to the load cancellation effects. In contrast to the horizontal force under the catenary systems, vertical force in the taut systems should be considered due to its significant influence on load capacity under inclined loads. As shown in Figure 5, the multiline potential of the MRA may impose larger forces on the vertical direction and a more extreme loading condition overall. Thus, reliable anchor design and determination of the extreme loading are required based on the multiline potential of the MRA.

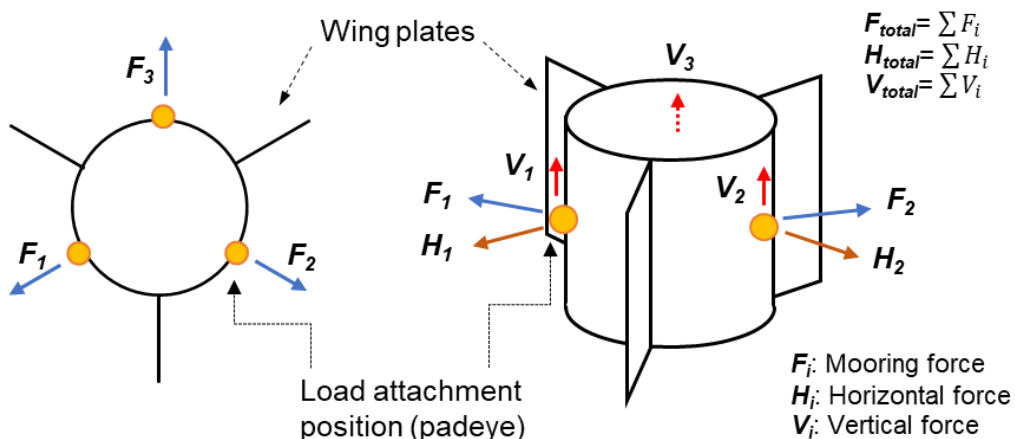


Figure 5. Extreme loading condition related to the multiline potential of the MRA

DETERMINATION OF THE EXTREME MOORING LOADS

Environmental condition. To determine the extreme taut mooring line loads, National Renewable Energy Laboratory's (NREL) FAST v.8 simulation tool is used. NREL 5-MW reference turbine and OC4 semisubmersible platform are considered for the 5-MW case study. Additionally, DTU 10-MW, the larger FOWT under extreme design load case, was also considered as a reference to further understand the scaled-up FOWT effects on anchor load demand (Bach-Gansmo et al. 2020). The load conditions considered for this study are shown in Table 1 below. In this scenario, the turbine will be in the parked and feathered condition in addition to the extreme wind and hydrodynamic loads. The turbulent wind fields were generated by Kaimal spectrum and the wave fields were generated using the JONSWAP spectrum. Currents are considered as steady and constant.

Table 1. Environmental conditions for mooring design under extreme conditions (Viselli et al. 2015)

Load case	Design load case (DLC 6.1)	Survival load case (SLC)
Conditions	Extreme non-operating	Survival non-operating
Wind speed at hub height	40 m/s (50-yr)	45 m/s (500-yr)
Significant wave height	10.2 m (50-yr)	12 m (500-yr)
Peak spectral wave	14.1 s	15.3 s
Current speed	0.45 m/s	0.55 m/s

Table 2. Properties of FOWTs, platform, and moorings (Robertson et al. 2014; Bach-Gansmo et al. 2020)

FOWT	NREL ^{a)} 5-MW	DTU ^{b)} 10-MW
Rotor diameter	126 m	178 m
Hub height	90 m	119 m
Rated speed	11.4 m/s	11.4 m/s
Platform	NREL OC4 Semisub.	NREL TetraSpar
Water depth/ radial distance	200 m/797 m	180 m/204 m
Taut angle	14.3°	44°
Line material	Braided polyester	Superline nylon

^{a)} National renewable energy laboratory

^{b)} Danish University of science and technology

Multiline anchor net force. The multiline configuration is obtained in a two-step process. First, the platform with three single lines are rotated, and second, the anchors are shared between lines. In this study, an anchor sharing three lines from three different turbine systems is considered. The three turbine systems are shown in Figure 6 below. These systems are analyzed with shared MRA for the extreme environmental condition discussed in the section above. Since the preliminary study shows that the maximum tension force occurs under the wind wave current (WWC) direction at zero degrees (Fontana et al. 2018), this study considered WWC=0° as shown in Figure 6. The vertical anchor forces from each of the contributing lines are shown in Figure 7a, which are color-coded as in Figure 6, and the vertical anchor force in the multiline condition is the time-domain resultant force superimposed from the three lines, as shown in Figure 7b. This force is considered as a base case to optimize and evaluate the uplift resistance of the MRA which will be discussed in the following section.

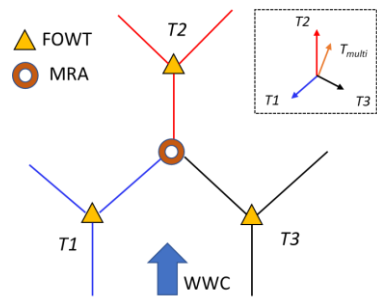
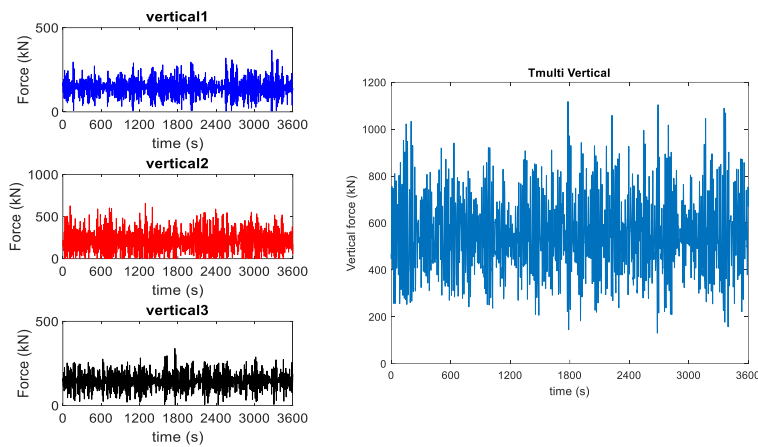


Figure 6. Multiline anchor net force (Balakrishnan et al. 2020)



(a) Individual lines (T_1 , T_2 , and T_3)

(b) Multiline (Resultant vertical force)

Figure 7. Vertical forces

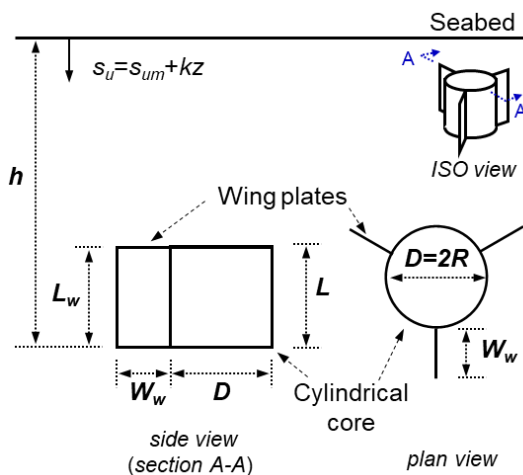


Figure 8. Dimensions of the MRA

Table 3. Anchor load demand

FOWT (load case)	NREL 5-MW (SLC)		DTU 10-MW (DLC 6.1)
	Mooring	Single-line	3-lines
$T_{v\text{-max}}^a)$ (kN)	703	1,176	1,180 ^{b)}
$F.S^c)$	1.05	1.05	2.0
Required axial capacity (kN)	738	1,235	2,360

^{a)} Maximum vertical force of the tension of the mooring line^{b)} Bach-Gansmo et al. (2020)^{c)} Factor of Safety (ABS 2015)

UPLIFT RESISTANCE OF THE MRA IN SOFT CLAY

In contrast to the catenary mooring systems, the taut mooring systems should consider combined horizontal-vertical loading (Figure 5). Additionally, mooring lines attached to the outside of the cylinder may induce added eccentric loading on the anchor. A prior study shows that the reductions in load capacity due to these rotational effects are tolerable (Aubeny and Lee 2020), and this has been identified as future research. Nevertheless, since the axial load capacity affect resultant load capacity as a major component under inclined loading (Aubeny 2003), evaluating the uplift resistance is critical for optimizing the MRA performance under the taut mooring systems. This axial capacity of the MRA can be enhanced by increasing the diameter of the cylindrical core, attaching wing plates, or increasing the embedment depth. These measures will be compared to the anchor load demand for each case to optimize the anchor performance (Table 3). The required anchor axial capacity can be computed based on the factor of safety ($F.S$), which varies depending on load cases. According to the anchor capacity guideline (ABS 2015), this study considered $F.S=1.05$ for the survival load case and $F.S=2.0$ for the extreme load case (Tables 1 and 3).

As a base case analysis for this study, a typical normally consolidated clay profile is selected, with a strength gradient $k=2\text{kPa/m}$ and mudline shear strength $s_{um}=5\text{kPa}$ (Quiros et al. 1983). The adhesion factor between pile and soil is taken as 0.7. This adhesion factor implicitly considers installation disturbance and setup, and can be considered appropriate for soils of low to medium sensitivity (Jeanjean 2006). The selection of an optimal aspect ratio L/D (Figure 8) is a subject of ongoing study but, for the present study, an aspect ratio $L/D=5/3$ is considered in all cases. All MRA designs have the same thickness ratio for each component (ring, wing plates, and stiffeners), $t_{ring}=t_{wing}=t_{sf}=D/120$. The diameter of the ring anchor varies from 2 to 4m, and wing plates, which width varying from $W_w/R=0$ (no wing) to $W_w/R=2$, are attached to the ring. A stiffener length $L_{sf}=1\text{ m}$ is used in all cases. For simplicity, when wings are attached to the MRA, a 3-wing configuration is used. Additionally, conventional suction caissons having the same diameter, same thickness ratio, and length $l=5D$ are considered as the base case for comparison to the MRA performance. Although the two anchors look similar, the difference in axial capacity mechanism between the two is significant. One of the components of uplift resistance of the conventional caisson is the reverse end bearing, while this does not exist for the MRA. The MRA cannot have comparable side resistance from the outer cylindrical surface due

to its relatively shorter length, but side skin friction along the inner surface of the MRA can partially offset these effects. Thus, the uplift resistance must be enhanced through other means such as optional wing plates or stiffeners to achieve parity with the caisson having the same diameter.

Table 4. Sources of uplift resistance for the MRA

Components	Equations	Assumptions	Sources
Ring	$V_{ring} = 2\pi D s_{u_MRA} (\alpha L + N_c t_{ring})$	Annular tip resistance factor, $N_c=9$	Randolph and Wroth (1978)
Wing plates	$V_{wing} = 2n_w W_w s_{u_MRA} (\alpha L_w + N_e t_{wing} + t_{wing} L_w / 2W_w)$	End bearing factor, $N_e=7.5$	Murff et al. (2005)
Stiffeners	$V_{stf} = 2N_{stf} D s_{u_stf} (\alpha L_{stf} + N_e t_{stf})$	End bearing factor, $N_e=7.5$	Murff et al. (2005)

where D = the diameter of the cylindrical ring, s_{u_MRA} = the average of the undrained shear strength for the MRA, s_{u_stf} = the average of the undrained shear strength for the stiffeners, α = the adhesion factor between anchor and soil, $L=L_w$ = length of ring and wing plates, and $t_{ring}=t_{wing}=t_{stf}$ = the thickness of the ring, wing plates, and stiffeners.

The MRA consists of an open tube, optional wing plates, and stiffeners (Figure 8), for which relatively simple equations exist for estimating load capacity. The vertical load capacity of the composite tube-plate geometry is possible by summation of the load capacity of the individual elements. Table 4 summarizes the equations and the main assumptions for each uplift resistance component. Keying flaps attached to the stiffener could further improve the vertical capacity of the MRA (Lee and Aubeny 2021). However, this is currently a focus of ongoing parallel research and will not be included in this study.

PARAMETRIC STUDY

To understand how the embedment depth, anchor size, and wing plates enhance the axial load capacity, this study investigates the effects of the parameters (Figure 8). From the standpoint of enhancing vertical load capacity of the MRA, the wing plates simply add more surface and end bearing area (e.i., additional areas by attaching wing plates; side: $n_w(2W_wL_w+t_{wing}L_w)$ and end bearing: $2n_w t_{wing} W_w$). Details of size and number of wings are relevant to the calculation; only the total areas matter. Therefore, the effect of the wing plates is best expressed in terms of a wing plate parameter, $n_w W_w / R$, where n_w is the number of wings, W_w is the width of the wings and R is the tube radius.

- Anchor size: the diameter of the core cylinder and length of the MRA, $D \& L$
- The embedment depth ratio, h/D
- The wing plate parameter, $n_w W_w / R$

Effect of the anchor size. In quantifying the effect of the anchor size on the axial load capacity, this study considers a single aspect ratio $L/D=5/3$. This value is actually based on consideration of MRA performance under horizontal loading, where prior studies show tolerable reductions in load capacity due to rotational effects (Lee and Aubeny 2020). Considering a single aspect ratio L/D and a single embedment ratio h/D , anchor uplift capacity varies as a cubic function of diameter D (Figures 9 and 10). Thus, increasing the anchor diameter is a highly effective means of gaining added load capacity for the anchor, although it obviously requires more steel, larger diameter anchors will likely require thicker

steel walls. The results show that uplift resistance increases with increasing anchor size at the same embedded depth h .

Effect of embedment depth. As noted earlier in Table 4, the uplift resistance is proportional to the soil strength in surrounding soils. Since undrained shear strength in a normally consolidated soil profile increases roughly linearly with depth, load capacity increases in a similar manner. In principle, embedding the MRA as deeply as possible is a highly effective means of increasing anchor load capacity without increasing the anchor dimensions. However, noting that suction installation is often the method of choice in soft clays (minimal required equipment, no acoustical impacts), this installation technique works only for embedment ratios $h/D = 6$. Additionally, penetration to $h/D = 6$ may be limited by site-specific soil conditions, so the possibility of lesser embedment depths needs to be considered. Figure 9 shows predicted trends. The effect of wing plates in this figure is for a base case scenario of three wings of width $W_w/R = 1$, or $n_w W_w/R = 3$. Aside from showing the relative influence of MRA diameter and embedment depth on vertical load capacity, Figure 9 shows that MRAs of modest dimensions ($D = 2-4\text{m}$) can easily resist vertical load demand for both the 5-MW base case considered in this study, as well as much larger (e.g. 10-MW) turbines that are contemplated in the near future.

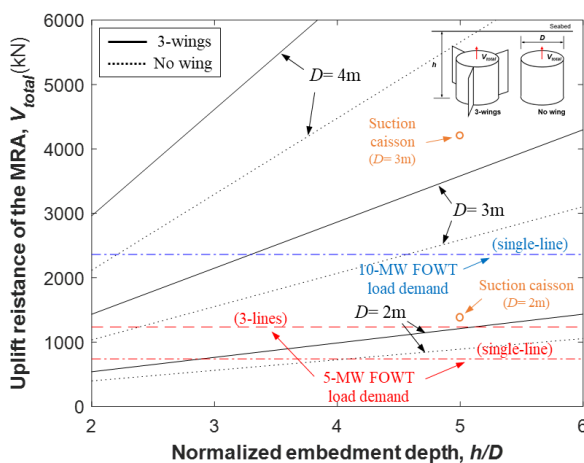


Figure 9. Effect of h/D on uplift resistance

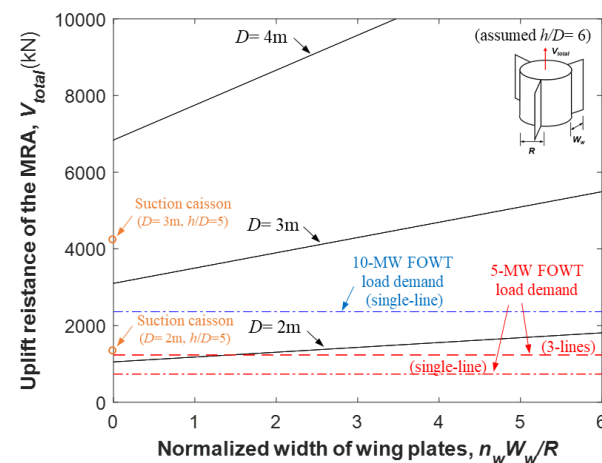


Figure 10. Effect of $n_w W_w/R$ on uplift resistance

Effect of the width of the wing plates. Vertical load capacity of the MRA is proportional to the side surface area and the end bearing area. Viewed purely from the standpoint of increasing uplift resistance, increasing the MRA diameter is just as effective as adding wing plates, so long as the anchors under consideration have the same surface and end bearing areas. Similarly, a small diameter MRA with wing plates requires the same amount of steel to achieve the same uplift capacity as a larger diameter MRA with no wings. However, the wing plates can confer substantial benefits in reducing transport and installation costs. Deck space requirements on a transport vessel are governed by the dimensions of the core tubular section of the MRA; thus, a smaller tube diameter means more anchors can be fit onto the vessel. Similarly, suction installation time is directly proportional to the interior volume of the tube, with a larger volume requiring a longer period of time to pump the water out. Thus, a wing plate design that reduces the interior volume of the caisson by 50% also reduces installation

costs by about 50%. Figure 10 shows that the wing plates can increase vertical load capacity by nearly 70% over a range $n_w W_w/R = 0\text{--}6$. Thus, wing plates offer a promising means of meeting the imposed load demand, while reducing transport and installation costs.

OPTIMAL DESIGN OF THE MRA IN SOFT CLAY

The high capital cost of the foundation system for the offshore wind farm can prevent a project from starting (Bhattacharya 2014). For this reason, optimal anchor design can play an essential role in reducing capital costs. Lee et al. (2020) presented that approximately 45 percent out of the foundation capital cost for the MRA installed in soft clay is material and fabrication costs. On the other hand, installation and transportation costs are about 8 percent out of the foundation cost. As the material and fabrication (M&F) costs are a direct consequence of the anchor size and as these costs are dependent on the unit steel price of bulk and unit fabrication price of bulk, indicative cost analyses based on total dry weight W_{dry} can be instructive in optimizing the anchor size (O'Loughlin et al. 2015). Figure 11 shows M&F costs of the MRA increase drastically with increasing the anchor size. On the other hand, the increase of the installation (Inst.) costs is relatively smaller than that of the M&F costs. Figure 12 illustrates that the required anchor size can vary depending on the embedment depth. Table 5 indicates that deeper installation can be a more cost-effective means with comparable uplift resistance compared to the bigger anchor size. Additionally, attaching wing plates can be an attractive solution to improve load capacity with comparable capital costs. Despite the approximate and indicative comparisons, this approach can allow useful insights to optimize the MRA design.

Additionally, the comparative study shows that the MRA can achieve comparable uplift resistance to conventional caissons by either wing plate attachments or deeper installation (Figures 9, 10, and 12). In addition, it has a clear advantage of significant capital cost saving (Figure 11). Therefore, the MRA can be a cost-effective alternative for securing FOWTs subjected to extreme conditions.

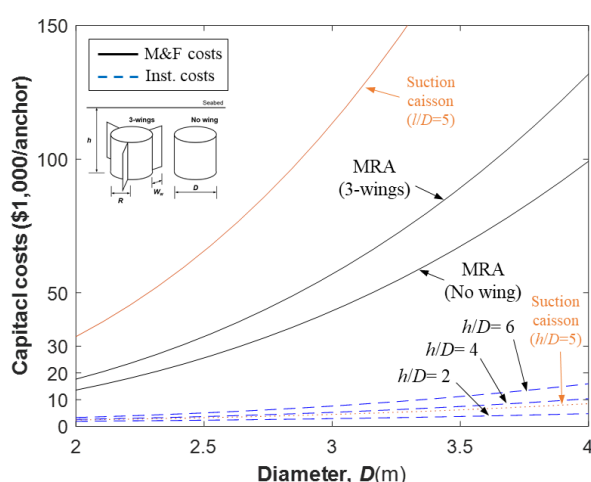


Figure 11. Total dry unit weight of the MRA

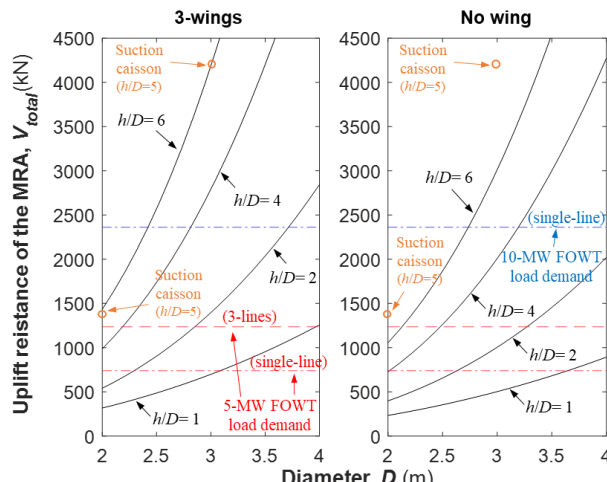


Figure 12. Optimal anchor design

Table 5. Optimal anchor design for 5-MW FOWT load demand (3-lines)

Anchor load demand	h/D	3-wings			No wing		
		Required D	M&F costs ¹⁾ (\$/anchor)	Inst. Costs ²⁾ (\$/anchor)	Required D	M&F costs (\$/anchor)	Inst. Costs (\$/anchor)
1,235 kN	2	2.72 m	42,884	2,552	3.23 m	53,440	3,243
	4	2.2 m	23,248	2,999	2.46 m	24,477	3,585
	6	1.83 m	13,720	2,909	2.13 m	16,255	3,706

¹⁾ M&F costs = Material cost + Fabrication costs, $Material cost (\$/anchor) = W_{dry} \times U_{steel}$, $Fabrication cost (\$/anchor) = W_{dry} \times U_{fab}$, where W_{dry} = Total dry weight of an anchor, U_{steel} = unit price of steel (\$/ton) U_{fab} = unit price of fabrication (\$/ton). U_{steel} is assumed as \$620/ton, and U_{fab} is assumed as \$3,500/ton for the cylinder \$2,500/ton for the plate part, respectively. (O'Loughlin et al. 2015; SteelBenchmark 2020).

²⁾ $Installation cost (\$/anchor) = t_{inst} \times U_{DR} \times (1/OW)$, t_{inst} = installation time per an anchor, U_{DR} = unit day rate of vessel (22,000\$/day) which cost includes fuel consumption, and OW = operation weather window (0 to 1). (Lee et al. 2020)

CONCLUDING REMARKS

This study presents a novel Multiline Ring Anchor (MRA) for floating offshore wind turbines (FOWT) and investigates its capabilities for use in taut mooring systems subjected to extreme loading conditions. The anchor can secure multiple mooring lines and was developed with a view toward reducing the capital costs of offshore wind farm development. Vertical load demand on the anchor is based on analyses for a 5-MW FOWT, but load demands from larger systems anticipated in the near future are also considered. While the MRA is deployable in a wide range of soils, the present study focuses on normally consolidated clays. Extreme loading conditions on large FOWTs can impose a large vertical load demand on the anchors. This study addresses whether an economically designed MRA is possible to resist these loads. Design measures for providing an MRA that can resist the load demand include increasing the anchor embedment depth, increasing the anchor diameter and adding wing plates (flanges) to the anchor. Embedding the anchor as deeply as possible into the seabed is a very effective means of increasing MRA capacity (Figure 9), but suction installation limits the maximum embedment depth to about $h/D = 6$. For a given MRA aspect ratio L/D and embedment h/D , MRA vertical load capacity varies with the cube of anchor diameter; thus, relatively modest dimensions of the MRA, say $D = 2-4$ m, are sufficient to resist vertical load demand imposed by a FOWT in an extreme event (Figures 9 and 10). If needed, wing plates can be added to the MRA to reduce the diameter of the core tubular section. This will not reduce material costs, but wing plates can significantly reduce transport and installation costs.

ACKNOWLEDGMENTS

The authors would also like to acknowledge the support from National Science Foundation, award number CMMI-1936901.

REFERENCES

Aubeny, C. (2017). *Geomechanics of Marine Anchors*, CRC Press, Taylor & Francis Group, Boca Raton, FL.

Aubeny, C. P., Han, S. W., and Murff, J. D. (2003). "Inclined load capacity of suction caissons." *International Journal for Numerical and Analytical Methods in Geomechanics*, 27(14), 1235-1254.

Aubeny, C. P., and Lee, J. (2020). "Horizontal Load Capacity of Multiline Ring Anchor in Soft Clay." *Proc., International Symposium on Frontiers in Offshore Geotechnics*, Austin, TX, USA.

Aubeny, C. P., Diaz, B. D., Arwade, S. R., DeGroot, D. J., Landon, M. E., Fontana, C., and Hallowell, S. T. (2020). Multiline Ring Anchor and installation method (U.S. Patent Application No. 16/978,760) U.S. Patent and Trademark Office.

ABS (American Bureau of Shipping). (2015). *Guide for Building and Classing-Floating Offshore Wind Turbine Installations*, American Bureau of Shipping, Houston, TX.

Bach-Gansmo, M. T., Garvik, S. K., Thomsen, J. B., and Andersen, M. T. (2020). "Parametric Study of a Taut Compliant Mooring System for a FOWT Compared to a Catenary Mooring." *Journal of Marine Science and Engineering*, 8(6), 431

Balakrishnan, K., Arwade, S. R., DeGroot, D. J., Fontana, C., Landon, M., and Aubeny, C. P. (2020). "Comparison of multiline anchors for offshore wind turbines with spar and with semisubmersible." *Journal of Physics: Conference Series*, 1452, 012032.

Barter, G. E., Robertson, A., and Musial, W. (2020). "A systems engineering vision for floating offshore wind cost optimization." *Renewable Energy Focus*, 34, 1-16.

Bhattacharya, S. (2014). "Challenges in design of foundations for offshore wind turbines." *Engineering & Technology Reference*, 1(1), 922.

Diaz, B. D., Rasulo, M., Aubeny, C. P., Fontana, C. M., Arwade, S. R., DeGroot, D. J., and Landon, M. (2016). "Multiline anchors for floating offshore wind towers." *Proc., OCEANS 2016 MTS/IEEE Monterey*, IEEE, 1-9.

Fontana, C. M., Hallowell, S. T., Arwade, S. R., DeGroot, D. J., Landon, M. E., Aubeny, C. P., Diaz, B., Myers, A. T., and Ozmutlu, S. (2018). "Multiline anchor force dynamics in floating offshore wind turbines." *Wind Energy*, 21(11), 1177-1190.

IEA. (2019). *Offshore Wind Outlook 2019*, IEA, Paris.

Jonkman, B., and Jonkman, J. (2016). "FAST v8. 16.00 a-bjj." National Renewable Energy Laboratory.

Lee, J., and Aubeny, C. P. (2020). "Multiline Ring Anchor system for floating offshore wind turbines." *Journal of Physics: Conference Series*, 1452, 012036.

Lee, J., Khan, M., Bello, L., and Aubeny, C. P. (2020). "Cost analysis of multiline ring anchor systems for offshore wind farm." *Proc., Deep Foundation Institute 45th Conference*, National Harbor, MD, USA, online, 484-493.

Lee, J., and Aubeny, C. P. (2021). "Effect of keying flaps on a Multiline Ring Anchor in Soft Clay." *Proc., International Foundation Congress & Equipment Expo*, Dallas, TX, USA, In press.

Lee, J., and Aubeny, C. P. (Forthcoming). "Lateral undrained capacity of a Multiline Ring Anchor in clay." *International Journal of Geomechanics*, DOI 10.1061/(ASCE)GM.1943-5622.0001995.

Murff, J., Randolph, M., Elkhatib, S., Kolk, H., Ruinen, R., Strom, P., and Thorne, C. (2005). "Vertically loaded plate anchors for deepwater applications." *Proc., Proc Int Symp on Frontiers in Offshore Geotechnics*, 31-48.

Musial, W., Heimiller, D., Beiter, P., Scott, G., and Draxl, C. (2016). *2016 Offshore Wind Energy Resource Assessment for the United States*. National Renewable Energy Lab (NREL), Golden, CO, USA.

O'Loughlin, C., White, D., and Stanier, S. (2015). "Novel Anchoring Solutions for FLNG- Opportunities Driven by Scale." *Proc., Offshore Technology Conference*, Offshore Technology Conference.

Quiros, G., Young, A., Pelletier, J., and Chan, J. (1983). "Shear strength interpretation for Gulf of Mexico clays." *Proc., Geotechnical practice in offshore engineering*, ASCE, 144-165.

Randolph, M. F., and Wroth, C. P. (1978). "Analysis of deformation of vertically loaded piles." *Journal of Geotechnical and Geoenvironmental Engineering*, 104(ASCE 14262).

Robertson, A., Jonkman, J., Masciola, M., Song, H., Goupee, A., Coulling, A., and Luan, C. (2014). *Definition of the semisubmersible floating system for phase II of OC4*. National Renewable Energy Lab (NREL), Golden, CO, USA.

Ruinen R. (2000). "The use of drag anchors and vertical loaded anchors (VLAS) for deep water moorings." *Continuous Advances in Mooring and Anchoring*. Aberdeen, Scotland.

SteelBenchmark. (2020). "Steel price history." <http://steelbenchmark.com/files/history.pdf>. Mar.26, 2020.

Viselli, A. M., Goupee, A. J., and Dagher, H. J. (2015). "Model Test of a 1:8-Scale Floating Wind Turbine Offshore in the Gulf of Maine1." *Journal of Offshore Mechanics and Arctic Engineering*, 137(4).